SUPPLEMENTARY DATA

Understanding the Influence of Copper on the color of glasses and glazes: copper environment and redox

Laurent Cormier[1], Cécile Noirot[1]

[1] Sorbonne Université, Muséum National d'Histoire Naturelle, UMR CNRS 7590, IRD, Institut de Minéralogie, de Physique des Matériaux et de Cosmochimie, IMPMC, 75005 Paris, France

❖ Copper-based pigments used at the Manufacture of Sèvres

Table S1. Copper-based pigments used at the Manufacture of Sèvres and referenced in d'Albis's book (d'Albis, 2003). The color corresponds to the description used at Sèvres.

	Color	**Description**	**Number1**	**Number2**	**Page**
Copper based pigment	Grey	$CuO + Fe_2O_3$, Mn_3O_4,Co_3O_4, NiO	10.132	1.298.61	211
Colored gold	red	CuO + Au (powder) the flux is bismuth sub-nitrate, $BiONO_3H_2O$			265
Colored underglaze for hard paste (CCPN = couverte colorée de pâte nouvelle)	**Dark green**	See below Table S2	**16**	**1.46.99**	300
	Green water	See below Table S2	**17**	**1.81.89**	300
	Dark green	Based on CCPN-16	25	1.200.90	300
	Turquoise celadon	CuO + uncolored underglaze + colored underglaze with Cr_2O_3	29	1.181.90	301
	Azur blue	CuO + uncolored underglaze + fritt with CoO	45	2.123.57	302
	Azur blue	Pigment 10.132 + uncolored underglaze + fritt with CoO	45 PC	1.11.77	302
	Blackish grey	CCPN-16 + pigments based on Fe and Mn	66	1.211.85	304
Glyceric colours	Fresh green	copper nitrate + glycerine	5	1.48.80	305
New paste enamels (émaux de pâte nouvelle)	Green enamel	$CuO + hard\ paste\ underglaze + Pb_3O_4 + SiO_2 + H_3BO_3$	19	1.17.55	308
	Green enamel	$CuO + SiO_2 + Pb_3O_4$	20 N	1.96.25	308
	Turquoise enamel	$CuO + SiO_2 + Pb_3O_4 + Na_2CO_3$	39 N	1.36.55	309
	Green celadon enamel	Pigment 20 N + pigment based on Fe	37 N		309
Background colors for soft paste	Yellow green	Copper chromate $CrCuO_4 + SiO_2 + Pb_3O_4$	9	1.329.26	315
	Olive green	$CuO + Fe_2O_3 + MnO$ + flux based on $SiO_2 + Pb_3O_4$	11	2.341.26	315
	Turquoise	CuO + flux based on $SiO_2 + Pb_3O_4$	12	2.301.46	315
	Light blue	$CuO + CoO$ + flux based on $SiO_2 + Pb_3O_4$	13	1.155.92	315
	Blue 'lapis'	$CuO + CoO + SiO_2 + Pb_3O_4 + Na_2CO_3$	21	1.147.27	316
	Jade	$CuO + Fe_2O_3 + NiO$ + flux based on $SiO_2 + Pb_3O_4$	24	1.142.48	316

	Turquoise	See below Table S2	**27 Ter**	**1.313.88**	**316**
	Camellia green	$CuO + Fe_2O_3$ + flux based on $SiO_2 + Pb_3O_4$	29	1.330.26	316
	Emerald green	$CuO + Fe_2O_3$ + flux based on $SiO_2 + Pb_3O_4$	30	1.190.85	316
	Leek green	$CuO + PbCrO_4$ + flux based on $SiO_2 + Pb_3O_4$	31	1.109.45	316
	Theodore Deck Green	Pigment 30 + Pigment 27ter		1.69.85	317
	Vincennes green	Pigment 38 + Naples Yellow (lead antimonate)	38	2.33.89	317
	Turquoise for 38	$CuO + H_3BO_3 + SiO_2 + Pb_3O_4 + Na_2CO_3$			317
	Egyptian blue	CuO + pigment 13 + $H_3BO_3 + SiO_2 + Pb_3O_4 + Na_2CO_3 + Li_2CO_3$	39	1.351.85	317
Stoneware colors	Yellow Brown-Greenish Streaks	$CuO + Fe_2O_3 + TiO_2$ + flux	20 G	1.165.24	322
	Black brown	$CuO + Fe_2O_3$ + uncolored underglaze + flux	21 G	1.77.69	322
	Greenish blue	$CuO + CoO + Fe_2O_3 + TiO_2$ + flux	24 G	1.248.00	322

CCPN: The mixture consists of a colorless matrix and CuO as pigment (d'Albis, 2003).

Glyceric colors: color, developed in 1939, which consists of the solution in glycerin of soluble metal salts

Hard paste enamels: it is a color applied in thickness and fired at 950°C (petit feu) on hard porcelain baked with its underglaze

Stoneware colors: these colors are still in used for hard paste porcelains.

Table S2. Composition of the three glazes investigated, as described in d'Albis's book (d'Albis, 2003).

	CCPN-16 - 1.46.99	CCPN-17 - 1.81.89	EPT-27ter - 1.313.88
Copper oxide	401	201	53
Chalk	1273	1528	
Finland feldspar	4221	4231	
Quartz BS 15	2645	2733	458
Kaolin BIP	1460	1307	
Sodium carbonate83%			201
Minium			288
	10000	10000	1000

❖ **Jahn Teller deformation**

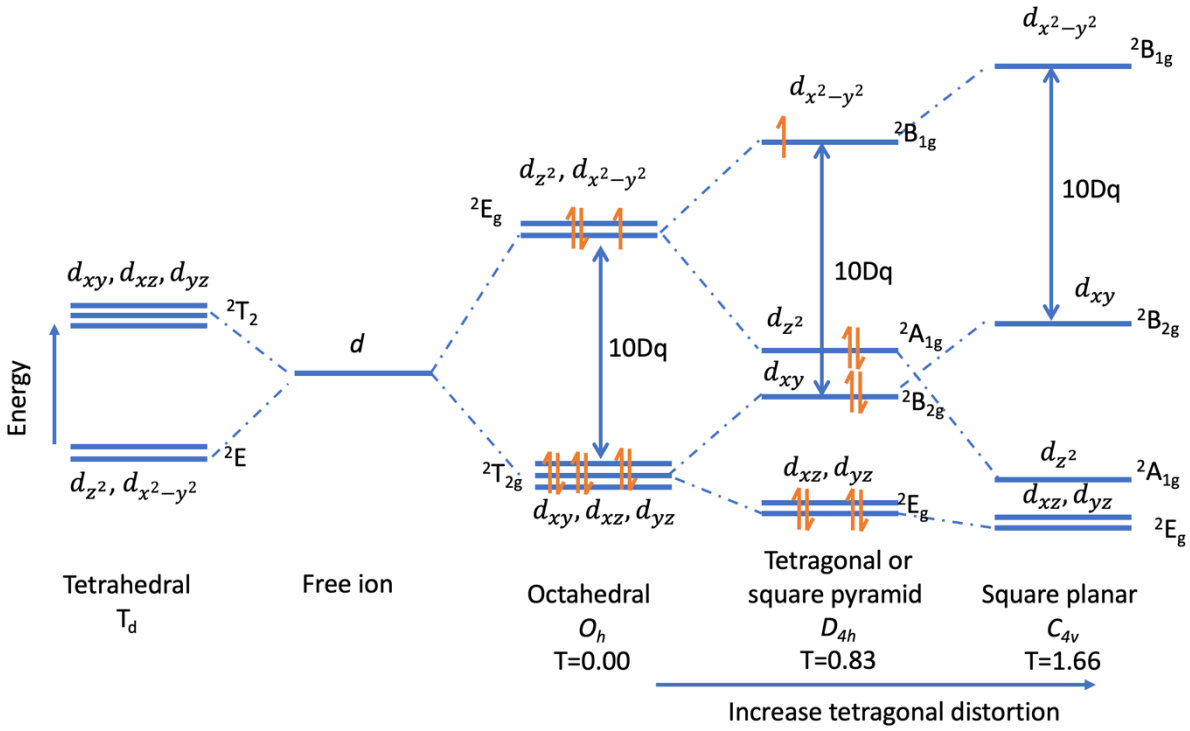

Figure S1. Energy level diagram of the Cu^{2+} ion in ligand fields with different symmetries.

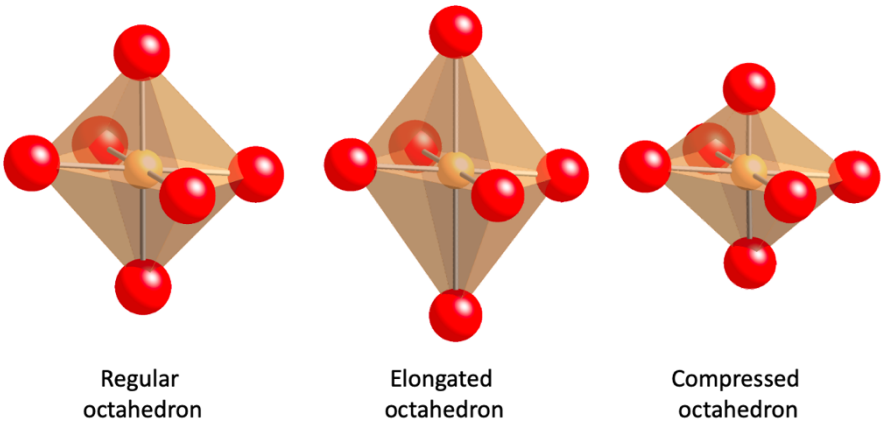

Figure S2. Representation of a perfect tetrahedron and Jahn-Teller distorted octahedra.

❖ Characterization of CCPN pigments and glazes

Before applying the glaze to the degourdi porcelain (Figure S3a), it is essential to conduct an initial firing of the porcelain at 850 °C, with a gradual temperature increase of ~100 °C per hour. This step ensures that porcelain paste gains solidity while preserving the necessary porosity for the subsequent glaze application. The water content within the raw porcelain, including that inherent in the kaolin sheets, is eliminated during this stage, leading to porcelain shrinkage due to water loss. In Figure S3b, the glaze has been applied and is now ready for the firing process. The grayish hue results from the black copper oxide present in the decorative mixture. After the firing process (Figure S3c), the color becomes permanently fixed onto the porcelain.

New hard paste colored covers (CCPN, derived from the French term '*Couverte Colorée de Pâte Nouvelle*') are prepared by grinding a colorless component with a specific chemical composition for new hard paste, along one or more pigments (refer to Tables S1 and S2). The grinding duration is tailored to the desired decoration and has been optimized by the chemists at the Manufacture of Sèvres. The colorless component, a vitrified coating named CI (derived from the French term '*Composant Incolore*'), is obtained from a mixture of feldspar, quartz, chalk and kaolin. The chemical composition of CI for the pigments relevant to the current study is provided in Table S2, as compiled by d'Albis (d'Albis, 2003). The CI and pigment(s) mixture is ground for 10 minutes at 300 rpm. Subsequently, the water is evaporated in an oven at 70 °C, resulting in a powder. The CCPN powders are then ready for immediate use or can be stored for future applications at the Manufacture.

Figure S3. (a) Example of colored coating deposition. (b) pre-fired condition. (c) Glaze after firing.

The firing procedure to achieve the glaze involves several stages: an initial temperature increase up to 300 °C within 3 hours, followed by a second rise up to 850 °C in 5 hours, and a final increase to 1280 °C over 4.5 hours with a 15-minute plateau. The gradual temperature rise ensures even distribution of temperature, a crucial factor, especially in the case of large furnaces. Following this firing process, the furnace is turned off, allowing for a natural cooling process. This gradual cooling is essential to prevent stress on both the porcelain and its glaze. The kiln atmosphere is not controlled during the firing of CCPN; instead, it relies on the

ambient, oxidizing air. This approach maintains an oxidizing atmosphere throughout the firing process.

X-ray diffraction (XRD) diagrams obtained on initial powders indicate that the mixture is predominantly amorphous. Identification of copper compounds is challenging, given the small amounts of CuO present, and only a weak Bragg peak attributed to unfused quartz is observed (Figure S4a). Following the firing process (Figure S4b), distinct Bragg peaks become visible. Given the highly fusible nature of the colorless glaze mixture, it is improbable that these peaks originate from the glaze itself, rather, they unquestionably result from the porcelain beneath the glaze. Similar to the starting mixture, no copper-related phases were detected.

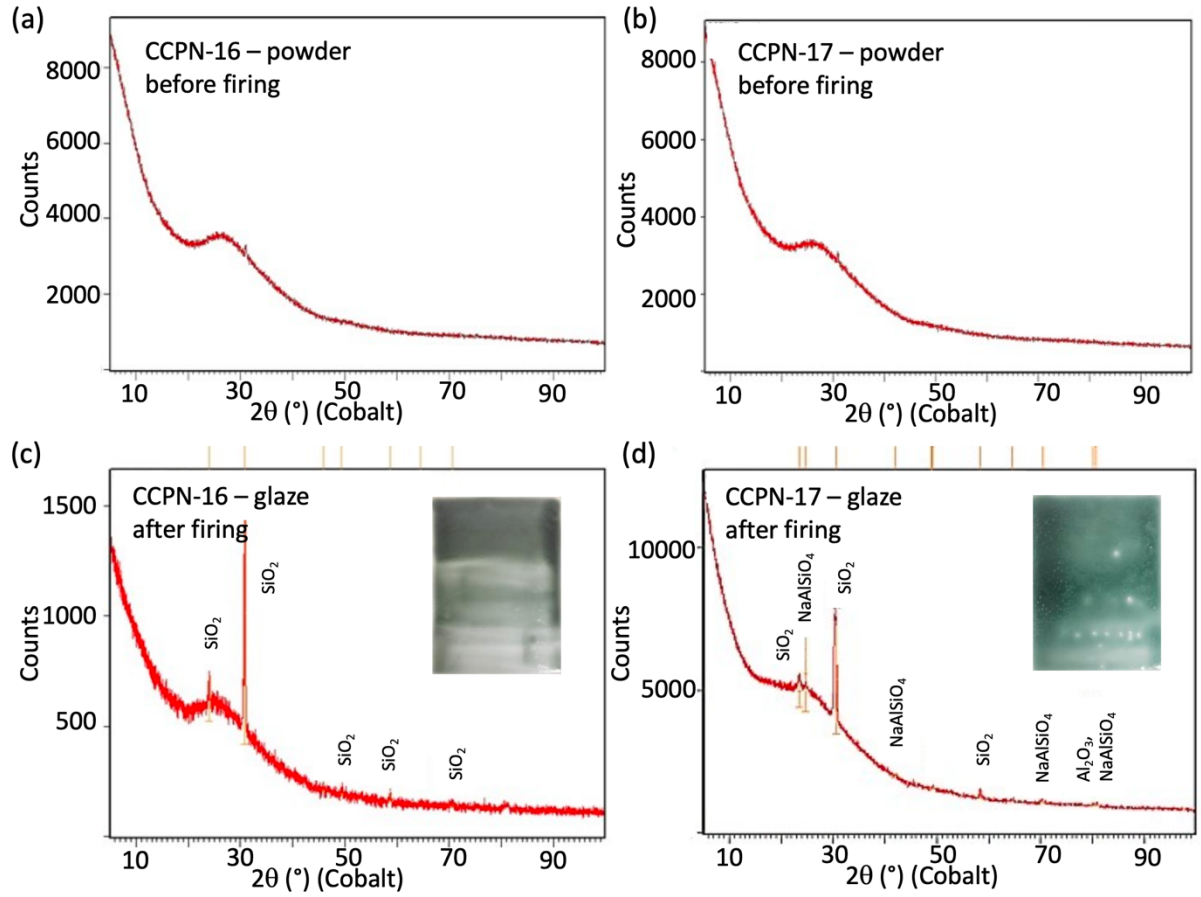

Figure S4. X-ray diffractograms of the initial powders of (a) CCPN-16 and (b) CCPN-17, prepared at the Manufacture of Sèvres. X-ray diffractograms of (c) the CCPN16 and (d) CCPN-17 glazes appplied on ceramic shards.

The glaze decorations were characterized using UV-visible spectroscopy. The diffuse reflectance spectra obtained were transformed into a remission function, F(r), through the application of the Kubelka-Munk formula (Kubelka and Munk, 1931).

Glaze decorations were applied in three different thicknesses to investigate the flaking limit of the enamel, while also exploring color hue variation with varying thickness. The optical absorption spectra corresponding to different thicknesses were normalized to the Cu^{2+} absorption peak near 12,600 cm^{-1} for comparative analysis. In the diffuse reflectance mode,

absorption intensity varies with grain size and our focus is on relative intensities. Unless specified otherwise, optical absorption spectroscopy will always be performed on the thickest part of the enamel.

The spectrum of the initial pigment CCPN-16 (Figure S5a, green curve) reveals the presence of an absorption edge near 14,500 cm^{-1}. This edge corresponds to the absorption by copper oxide mixed with the colorless component CI. The spectrum for CCPN-16 glaze shows the emergence of a band in the visible range around 12,600 cm^{-1} (Figure S5a, red curve), explaining the green color and corresponding to Cu^{2+} ions occupying tetragonally distorted octahedral sites (refer to the main text). Absorption is lower for the region between 15,000 and 20,000 cm^{-1}. A second band appears in the near UV region around 27,000 cm^{-1} and extends towards the visible. Iron, present as an impurity in quartz, is the most likely candidate to explain the appearance of the UV band. At these energies, there are three absorption bands located near 22,800, 24,000 and 26,400 cm^{-1}, that are attributed to Fe^{3+} ions, and an intense oxygen-iron charge transfer band (Vercamer, 2016). This UV band also contains various contributions due to Cu^{+} and charge transfers (see main text). The glaze exhibits a green tint after firing above 1,100°C on the ceramic shard Figure S5b.

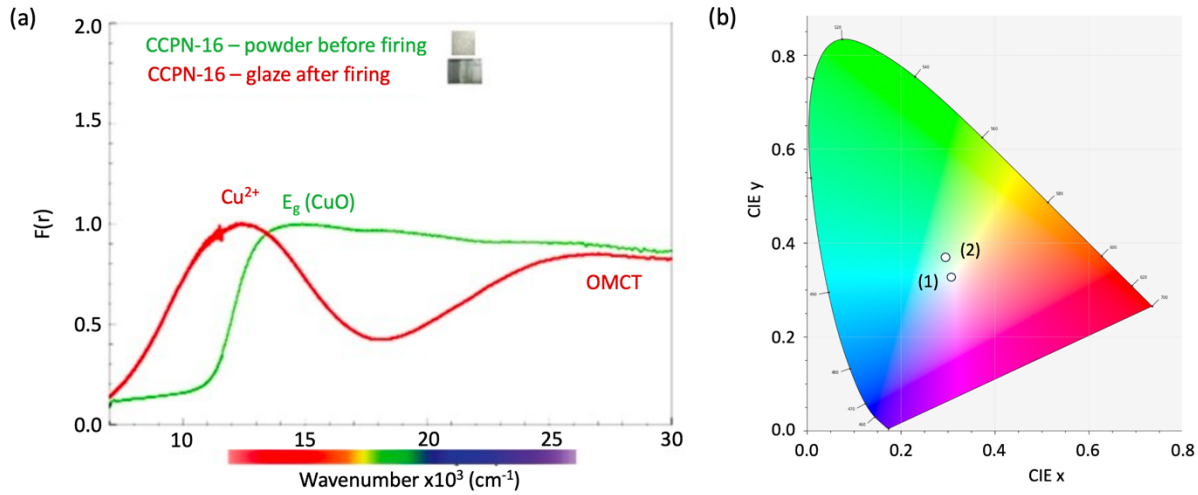

Figure S5. Optical spectroscopic results for CCPN-16. (a) Optical absorption spectra for the initial powder (green) and the glaze applied on the ceramic (red). (b) Chromaticity diagram, where pigment color coordinates are calculated from their diffuse reflectance spectra. Points 1 and 2 correspond to the initial powder and the glaze applied on the ceramic, respectively.

Figure S6 presents optical absorption spectra measured in three different regions corresponding to varying glaze thicknesses for CCPN-16. The Cu^{2+} band widens with increasing thickness and, consequently, with the intensity of the color (A > B > C).

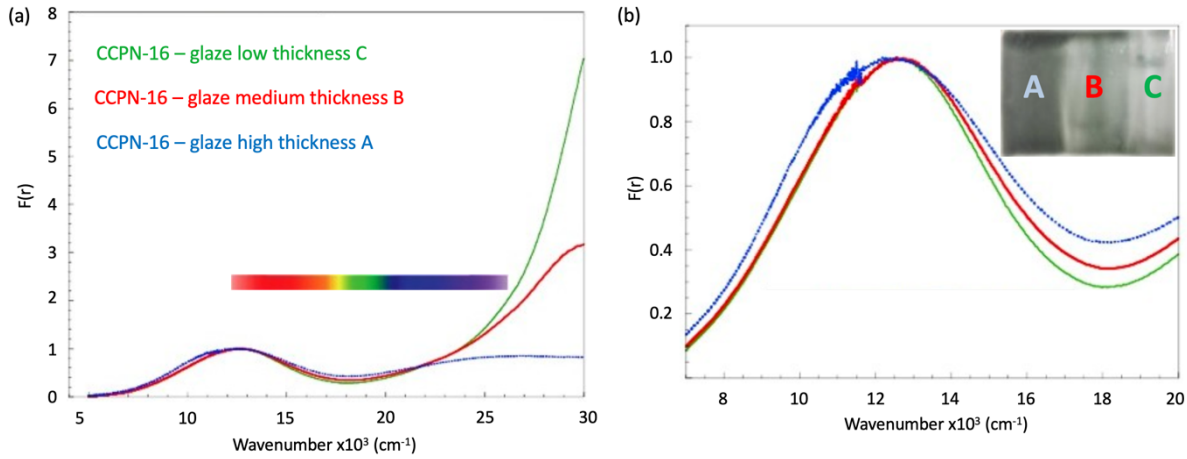

Figure S6. (a) Optical absorption spectra obtained on the three regions of the ceramic shard corresponding to varying thicknesses of the glaze. (b) Zoom on the Cu^{2+} absorption band.

CCPN-17 exhibits nearly identical characteristics to CCPN-16. Figure S7 shows the CuO absorption edge for the initial powder before firing and the two bands absorption bands in the glaze, primarily due to Cu^{2+} and charge transfer bands associated with Fe^{3+} and Cu^{+}. The thickness effect remains consistent with CCPN-16 in the broadening of the Cu^{2+} band, and it is not represented as it does not provide new information.

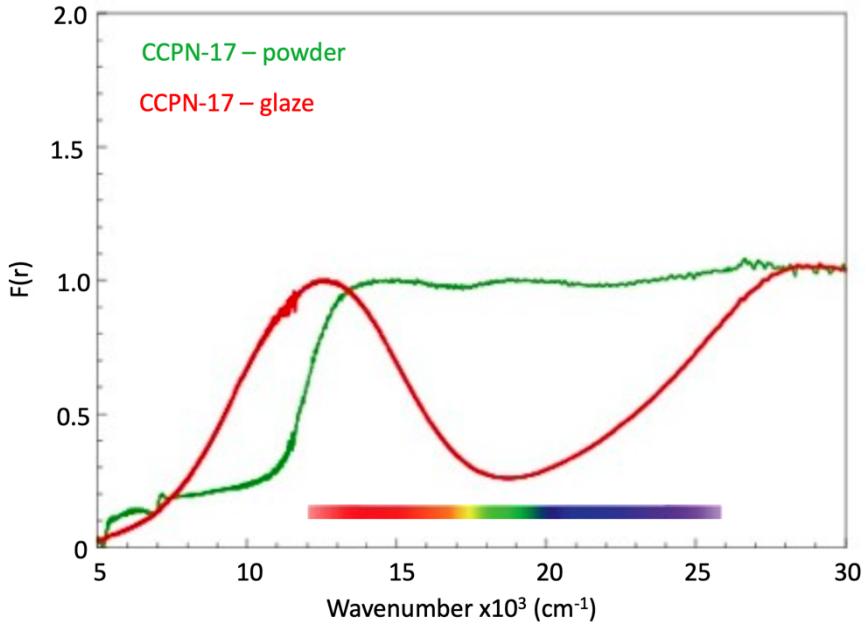

Figure S7. Optical absorption spectra for CCPN-17: initial powder (green) and the glaze applied on the ceramic (red).

❖ Characterization of EPT pigments and glazes

The glaze for the soft porcelain is predominantly composed of a lead silicate. To achieve aesthetic results after firing, it must be applied with a specific thickness. Given its tendency to flow on vertical surfaces, it is essential to include a refining stage at the end of the firing process. This additional step allows the glaze, especially in areas where it has accumulated, sufficient time to refine, facilitating the escape of air or gas bubbles. The glaze is fired at 880 °C, with a two-hour refining stage observed at the end of the firing process.

The third pigment mixture considered in the current study is the EPT-27ter, a lead silicate glass. Lead serves as a flux, aiding in the homogenization and diffusion of elements during the firing process. Table S2 provides the composition of the EPT-27ter.

The XRD diagram in Figure S8a shows that EPT-27ter has a completely amorphous structure as expected due to high fusibility of the lead silicate. In the optical spectrum of EPT-27ter (Figure S8b), two absorption bands are present, one centered at 12,700 cm^{-1} and another one at 28,600 cm^{-1}. The minimum absorption is distinctly localized in the blue region, differing from the CCPN glaze where the minimum was red-shifted, resulting in a greenish coloration.

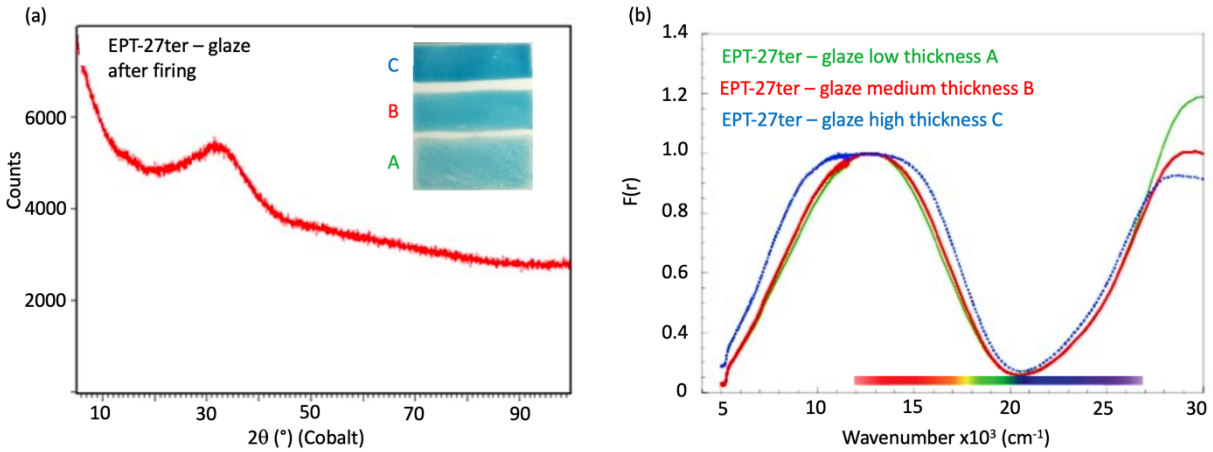

Figure S8. (a) X-ray diffractogram of the EPT-27ter glaze appplied on a ceramic shard. (b) Optical absorption spectra obtained on the three regions of the ceramic shard corresponding to varying thicknesses of the glaze.

To investigate the impact of melting temperature on the coloration of EPT-27ter, normally fired at 880 °C at Sèvres, the EPT-27ter mixture was remelted at 1250 °C in a platinum crucible for one hour. Following this heat treatment, the bottom of the crucible was immersed in water to quench the glass. Pieces of glass were then polished with parallel faces to avoid any background absorption. The optical absorption spectra in Figure S9a were obtained in transmission mode. It is observed that there is a sharp reduction in intensity when the firing temperature increase. The two bands are centered around 1200 cm^{-1}. On the chromaticity diagram it is noticeable that for melting at 1250 °C, there is a shift towards the green region, which is visually confirmed in the sample photos. The color variation in these two samples

seems to result from both the variation in the Cu^{2+} absorption band and the UV band, indicating a different copper redox state. Lead-based glass exhibits a clearly distinct behavior from the CCPN samples.

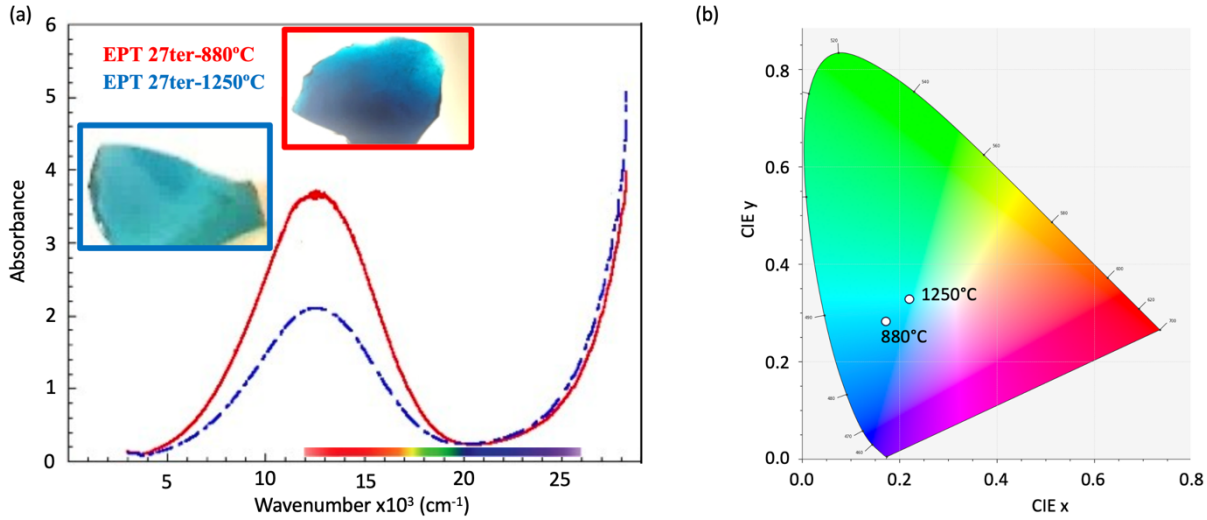

Figure S9. Effect of the melting temperature on (a) the optical absorption spectra and (b) the corresponding points in the chromaticity diagram.

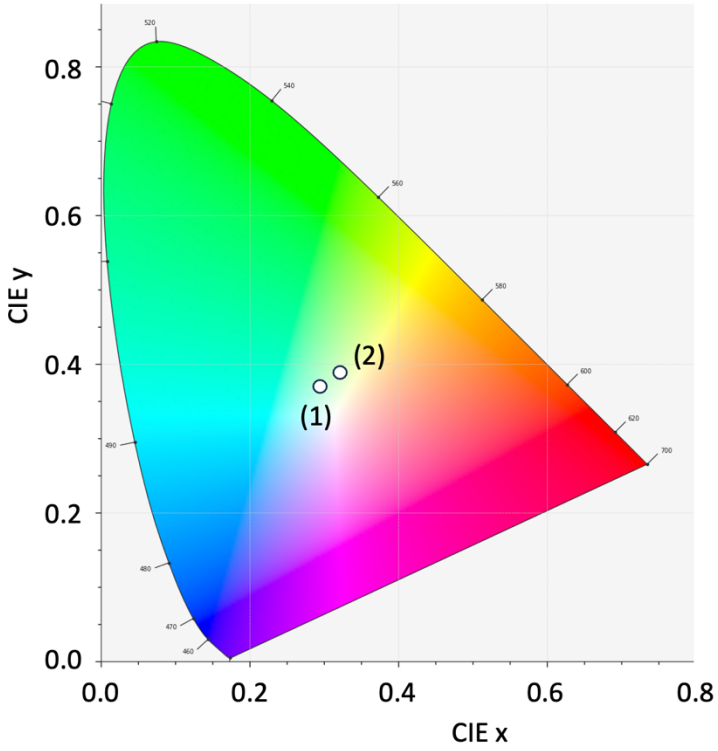

Figure S10. Chromaticity diagram where points 1 and 2 stand for CCPN-16 and CCPN-17 glazes, respectively.

❖ Density measurements of glazes

The densities of the glasses are measured using a hydrostatic balance, which measures the Archimedes's thrust. The process involves weighing a glass piece in air (m_{air}) and then the same piece, immersed in ethanol of known density, (m_{liquid}). The density is calculated using the formula:

$$\rho_{glass} = \rho_{ethanol}(T)\frac{m_{air}}{m_{air} - m_{liquid}}$$

Multiple pieces without cracks or bubbles are measured and the average values are reported in Table S3. The density of CCPN-17 is slightly underestimated due to the presence of small bubbles.

Table S3. Densities of the glazes.

	BX9	CCPN-16	CCPN-17	EPR-27ter 880 °C	EPR-27ter 1250 °C
Density (g.cm^{-3})	2.56 ± 0.01	2.45 ± 0.01	2.3 ± 0.01	3.29 ± 0.01	3.24± 0.01

❖ **Copper content in glasses**

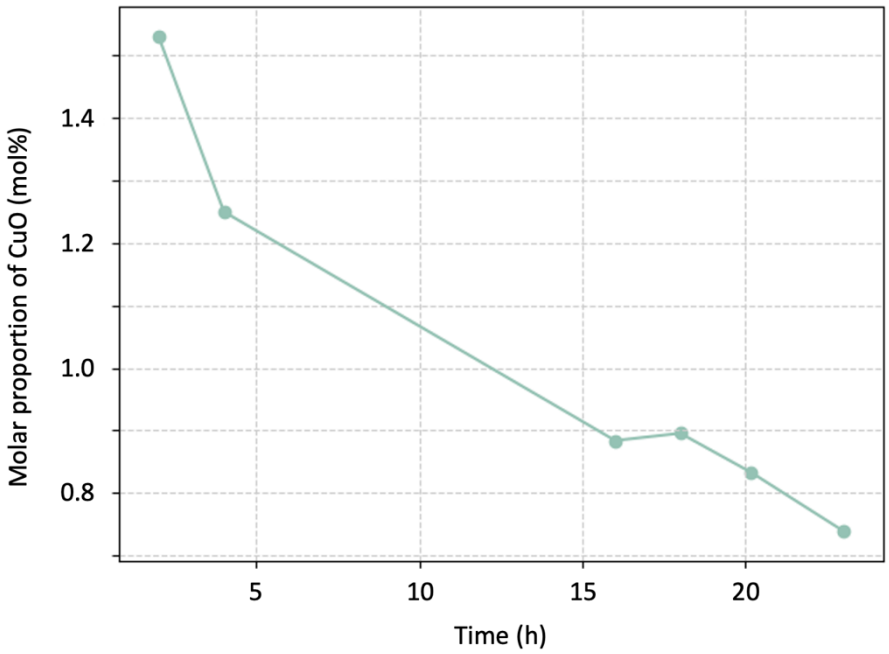

Figure S11. Proportion of copper (mol%) measured by EPMA against the melting time for CCPN-17.

Table S4. Proportion (mol%) of FeO determined through EPMA in Sevres samples.

	CCPN-16	CCPN-17	EPT-27ter 880°C	EPT-27ter 1250°C	BX9
FeO content (mol%)	0.12(4)	0.11(1)	traces	traces	0.05(4)

❖ **Fit of the optical absorption spectra**

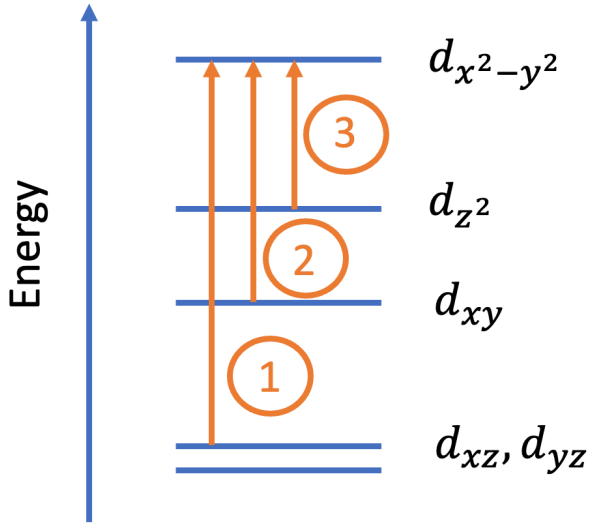

Figure S12. Number for the transitions used in the fitting of the Cu^{2+} absorption band.

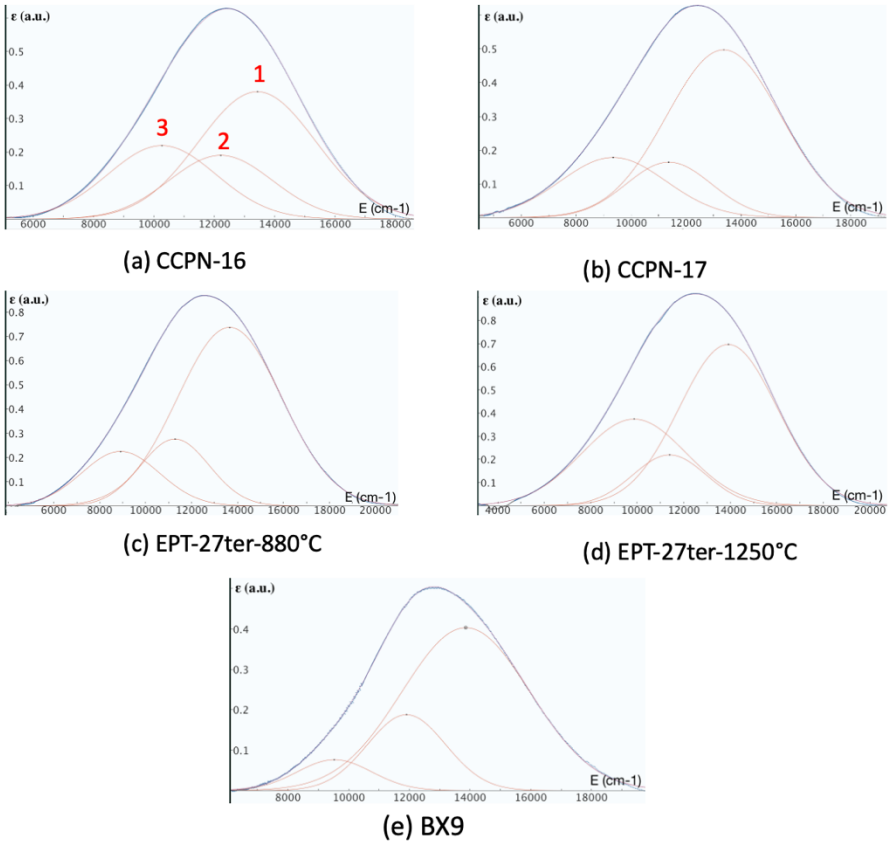

Figure S13. Fit of the Cu^{2+} absorption band comparing the experimental spectra (blue curves) with the three Gaussian functions (red curves). A straight line was used for the baseline. Though not significantly changing the trend, it would be more accurate to use the tail of a Gaussian, with the maximum positioned in the UV.

❖ **Fit of the EPR spectra**

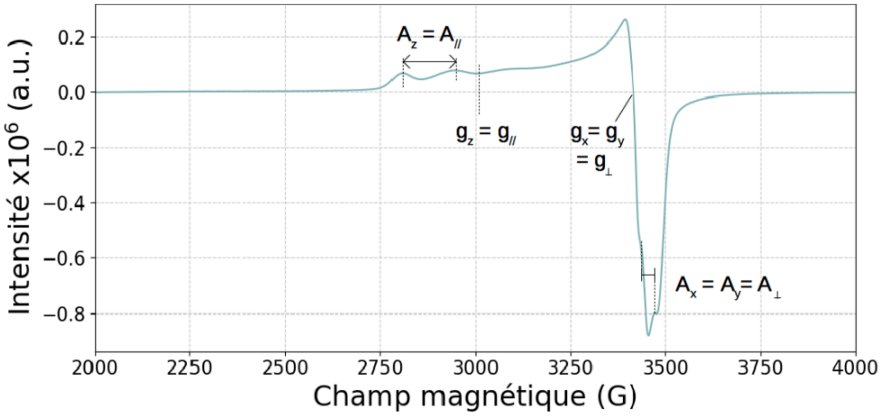

Figure S14. EPR spectrum for BX9 showing the EPR parameters in axial symmetry.

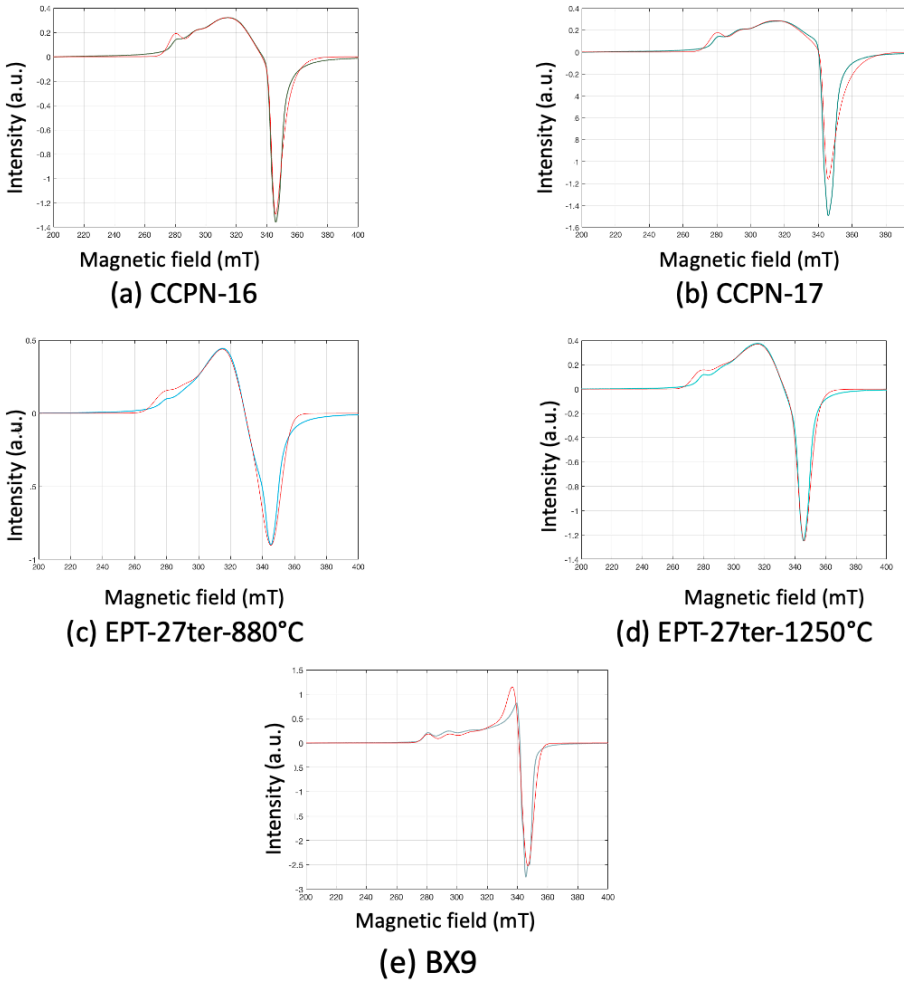

Figure S15. Comparison of the experimental EPR spectra (blue curve) with the fit (red curve).

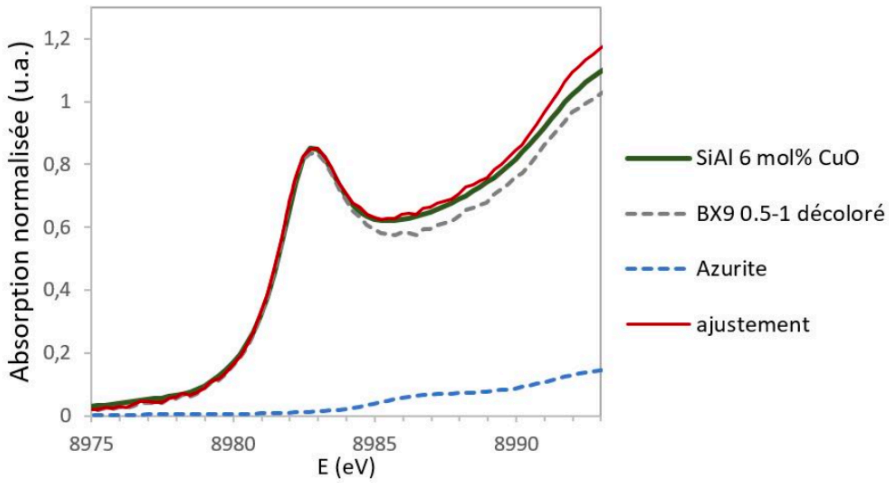

Figure S16. Example of fit of the XANES spectra at the Cu K-edge using two references: azurite, $Cu_3(OH)_2(CO_3)_2$, for Cu^{2+} and a glass of known redox for Cu^{+}.

References

d'Albis, A., 2003. Traité de la porcelaine de Sèvres. Faton, Dijon, France.

Kubelka, P., Munk, F., 1931. Ein Beitrag zur Optik der Farbanstriche. Z Techn Phys 12, 593–601.

Vercamer, V., 2016. Spectroscopic and structural properties of iron in silicate glasses (PhD Thesis). Université Pierre et Marie Curie - Paris VI, Paris.